JACS
JOURNAL OF THE AMERICAN CHEMICAL SOCIETY

Communication

pubs.acs.org/JACS

Thermodynamics of Electron Flow in the Bacterial Deca-heme Cytochrome MtrF

Marian Breuer,[†] Piotr Zarzycki,[‡] Jochen Blumberger,*[,†] and Kevin M. Rosso*[,§]

[†]University College London, London, United Kingdom

[‡]Institute of Physical Chemistry, Polish Academy of Sciences, Warsaw, Poland

[§]Pacific Northwest National Laboratory, Richland, Washington, United States

Supporting Information

ABSTRACT: Electron-transporting multi-heme cytochromes are essential to the metabolism of microbes that inhabit soils and carry out important biogeochemical processes. Recently the first crystal structure of a prototype bacterial deca-heme cytochrome (MtrF) has been resolved and its electrochemistry characterized. However, the molecular details of electron transport along heme chains in the cytochrome are difficult to access via experiment due to the nearly identical chemical nature of the heme cofactors. Here we employ large-scale molecular dynamics simulations to compute the redox potentials of the 10 hemes of MtrF in aqueous solution. We find that as a whole they fall within a range of ~0.3 V, in agreement with experiment. Individual redox potentials give rise to a free energy profile for electron transport that is approximately symmetric with respect to the center of the protein. Our calculations indicate that there is no significant potential bias along the orthogonal octa- and tetra-heme chains, suggesting that under aqueous conditions MtrF is a nearly reversible two-dimensional conductor.

Metal-respiring bacteria utilize a complex network of electron-transfer (ET) proteins to transport electrons from their inner membrane across the periplasm and the outer membrane toward extracellular substrates.[1] The latter include solid metal oxides like ferrihydrite and manganese dioxide.[2,3] Electron transport may cover distances of several micrometers along conductive pili via ET proteins as central constituents,[4,5] probably by multi-step charge hopping.[6] These ET proteins are thus interesting not only in the biological context but also because they show promise in nano-biotechnological applications.[7,8]

Recently Clarke et al.[9] published the first crystal structure of an outer-membrane ET protein from a metal-respiring bacterium, the deca-heme c-type cytochrome MtrF from *Shewanella oneidensis*. Like homologue MtrC, MtrF is proposed to help facilitate the final steps of electron transport across the outer membrane to extracellular substrates, in cooperation with a periplasmic cytochrome MtrD and a membrane barrel protein MtrE, which is proposed to enable contact for electron transfer between MtrD and MtrF (see Figure 1). MtrF is assumed to pass electrons on to extracellular substrates.

The crystal structure of MtrF is shown in Figure 1. It consists of four domains, with domains I and III containing β-sheets and

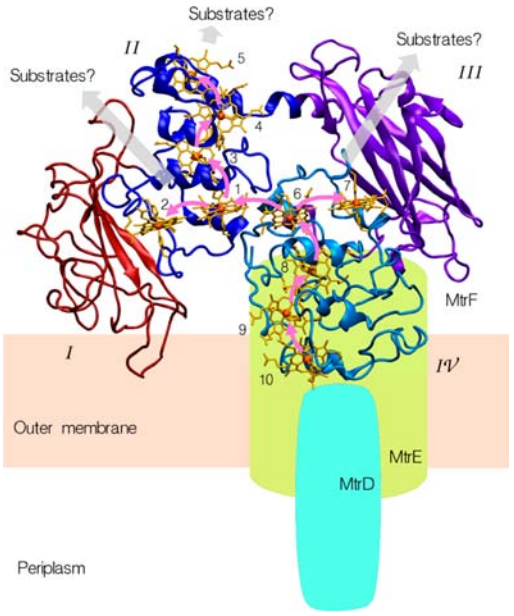

Figure 1. The protein MtrF, its proposed location on the outer membrane of *S. oneidensis*, and its interaction with the proteins MtrE and MtrD. Hemes are numbered with arabic, domains with roman numerals. Iron atoms are shown in orange.

domains II and IV α-helices. The latter two domains each bind five heme c-cofactors, covalently bound to the protein via two cysteine linkages in a CXXCH binding motif (C, cysteine; H, histidine; X, arbitrary residue) and ligated by two histidines. The heme cofactors are arranged in a "staggered cross" formation, with the four roughly coplanar hemes 2, 1, 6, and 7 in the center of the protein and the heme triples 3, 4, 5 and 8, 9, 10 being nearly parallel-stacked and placed perpendicular to the central heme plane. This arrangement yields an octa-heme chain between hemes 5 and 10, with hemes 1 and 6 as branching points toward hemes 2 and 7, respectively.

While the protein crystal structure has been characterized, many aspects of the function of the protein, including the thermodynamics and kinetics of electron transport, as well as the binding sites for electron acceptors, are largely unknown. The 10 heme redox potentials were reported to range from 0 to

Received: March 21, 2012
Published: June 4, 2012

dx.doi.org/10.1021/ja3027696 | *J. Am. Chem. Soc.* 2012, 134, 9868–9871

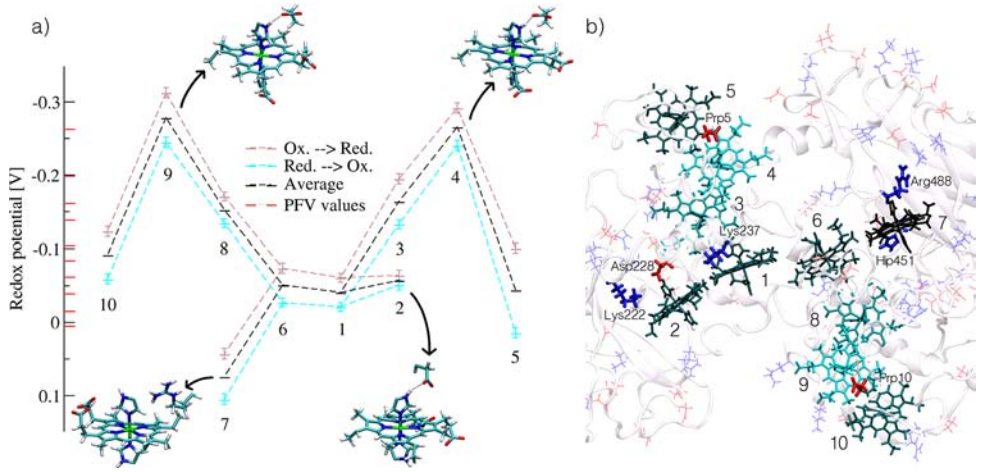

Figure 2. Redox potentials for the heme cofactors in MtrF. (a) Redox potentials for each cofactor in both directions of thermodynamic integration, together with their averages. Values from protein film voltammetry are shown on the left edge in red. (b) MtrF with hemes colored from light green (low redox potential) to black (high redox potential). Negatively and positively charged residues are shown in red and blue, respectively. Important residues discussed in the text are highlighted.

−0.260 V for solvated MtrF and between −0.044 and −0.312 V from protein film voltammetry (values relative to the normal hydrogen electrode).[9] No assignments of these values to individual hemes have been reported, hindered by the nearly identical chemical nature of the 10 hemes. The heme-to-heme ET free energy landscape along chains in MtrF thus remains obscured. Yet, the elucidation of this profile is of high importance as it is key to our understanding of the energetics of electron transport across and between microbial cells, a subject of intense recent interest.[1,4,8,9] It also provides much needed input parameters for kinetic models for electron transport across MtrF and along conductive microbial pili that were suggested very recently.[6]

The simulation of redox and ET reactions in mono-heme cytochromes has been the subject of successful computational studies, including the calculation of redox potentials,[10,11] reorganization energies,[12−18] and electronic couplings.[19,20] These investigations paved the way for applications to larger and more complex cytochromes. Here we use large-scale molecular dynamics (MD) simulations to compute heme microscopic redox potentials for the deca-heme protein MtrF, which allows us to construct the desired free energy landscape for electron transport through this protein. We find an almost symmetric free energy profile with only small differences in the redox potentials of the terminal hemes, implying that electron transport across the protein is nearly reversible.

We consider the case where electron supply to MtrF is limited so that all cofactors $j \neq i$ are in the oxidized state except heme i that carries the excess electron. The free energy for oxidation of the latter, ΔG, was calculated using a standard thermodynamic integration protocol,

$$\Delta G = \int_0^1 \left\langle \frac{\partial E_\eta}{\partial \eta} \right\rangle_\eta \mathrm{d}\eta \qquad (1)$$

where $(\partial E_\eta/\partial\eta) = E_O - E_R + (2\eta - 1)E_\Delta$, E_O and E_R are the potential energies of MtrF in the all-oxidized state and in the state where heme i is reduced, respectively, and E_Δ is a small energy term due to the integration path chosen (see SI for details). The coupling parameter η takes values from 0 (= Fe(II) heme i) to 1 (= Fe(III) heme i). Since all 10 heme cofactors of MtrF are chemically identical, one can assume that most of the difference in heme redox potentials is due to the electrostatic effect of the protein and solvent. This implies that classical force fields should be suitable for calculating redox potentials. Of course, any more subtle effects such as electronic polarization of the heme cofactors due to the environment are neglected in this approach. However, previous QM/MM calculations on cytochrome c indicated that such effects are small.[16] In this regard and in view of the long simulation times needed to obtain converged averages, we preferred in this study to use classical MD simulation over QM/MM. The atomic partial charges for the reduced and the oxidized heme cofactors were parametrized previously by carrying out density functional theory calculations on gas-phase Fe(II)- and Fe(III)-porphyrin-(imidazole)$_2$.[18,17] Thus, all atoms of the porphyrin ring and axial histidine ligands are subject to a change of charge during oxidation. The protein was modeled using the AMBER03 force field parameters[21] for both oxidation states. An initial structure for the protein simulation was prepared by solvating the crystal structure of MtrF in 0.1 M NaCl and choosing protonation states according to pH 7. The integral eq 1 was approximated by a finite sum using η = 0.0, 0.25, 0.50, 0.75, and 1.00. For each window MD simulations were carried out. After 2.75 ns of equilibration, the vertical ionization potential was averaged over a trajectory of length 2.75 ns. Simulations were carried out from the oxidized to the reduced state $(1.0 \rightarrow 0.0)$ and in the reverse direction $(0.0 \rightarrow 1.0)$ for each of the 10 hemes. Free energies for oxidation were converted to redox potentials ε via $\Delta G = F\varepsilon$, where F is the Faraday constant. The computed absolute redox potentials cannot be directly compared to the experimental redox potentials but are offset from the latter by a cofactor-independent constant C, which depends on the charge parametrization of the cofactors and the boundary conditions for which the derivative $(\partial E_\eta/\partial\eta)$ is computed (see ref 22 for a more detailed explanation of the last point.) The constant C was determined by sorting computed and experimental redox potentials in ascending order and choosing C such that the sum of the square differences between computed and experimental redox potentials is minimal. This procedure gave C = −1.567 V. Thus, the shape of the free energy profile, i.e., the relative heme reduction potentials $(\Delta\varepsilon)$, can be obtained from the MD

dx.doi.org/10.1021/ja3027696 | J. Am. Chem. Soc. 2012, 134, 9868−9871

simulations, whereas the absolute zero of the potential is adjusted empirically.

The redox potentials obtained for each cofactor are shown in Figure 2a and summarized in Table S1. The position of the hemes in the protein is shown in Figure 2b, where cofactors are colored according to their redox potential from light green (= lowest redox potential = highest free energy in Figure 2a) to black (= highest redox potential = lowest free energy). As the 10 heme redox potentials fall within a narrow range of only ∼0.3 V, we first discuss the statistical uncertainties of our simulations. We find that the free energy derivative $(\partial E_\eta/\partial\eta)$ is converged within a few ns of simulation time (Figure S1). The corresponding error bars due to the finite length of the trajectories are displayed for each data point in Figure 2a. They are <0.01 V, and for all practical purposes negligible. The deviation between forward and backward thermodynamic integration (brown vs blue line in Figure 2a) is larger. We have taken the average over the two directions as final redox potentials and half of the differences as the final uncertainties. The latter are typically not larger than 0.03 V and significantly smaller than the redox potential differences between adjacent hemes (0.1−0.2 V), except for the group of hemes 6-1-2 which lie within a very narrow potential range (0.02 V). Overall, we can conclude that the uncertainties of our simulations are sufficiently small, permitting the construction of a statistically significant free energy profile.

We find that the computed potential range (0.35 V) is somewhat larger than in experiment (0.26 V). Assuming partial deprotonation of a protonated histidine in the vicinity of heme 7, the computed potential range decreases to 0.29 V, in very close agreement with experiment. Comparison with experiment should be considered with some caution, however, since the computed values are microscopic redox potentials relevant for one-electron transport through all-oxidized MtrF, whereas experimental values are macroscopic potentials for accumulated stepwise reduction of the protein. Notwithstanding this difference, the relatively good reproduction of the experimental range can be seen as a first validation of our simulation methodology.

The free energy landscape shown in Figure 2a is roughly symmetric with respect to the protein center (except for the heme pair 7 and 2). This is not very surprising if one considers the approximately symmetric arrangement of penta-heme domains II and IV in MtrF (Figure 2b). The free energy landscape comprises two "hills" (10-9-8-6 and 1-3-4-5), with hemes 6 and 1 forming a plateau. The redox potential of heme 10, hypothesized to receive an electron from MtrE in the bacterial MtrDEF complex,[9] is only ∼0.05 V lower than that of heme 5 at the other end of the octa-heme chain, and 0.04 and ∼0.09 V lower than those of hemes 2 and 7 at the termini of the tetra-heme chain (assuming partial deprotonation of the histidine in the vicinity of heme 7, see below and SI). Unfortunately, experimental assignments of redox potentials are not available (yet) to verify our theoretical predictions. However, it seems plausible that the redox potentials of the terminal hemes of MtrF are similar such that loss of free energy during electron transport across the protein is minimal. Clearly, the advantage of a symmetric free energy profile over a simple downhill slope is that electrons can flow reversibly, albeit at the expense of slower forward ET rates. The small potential differences at the termini also mean that the computed redox potentials do not give a hint regarding likely electron entry/exit sites into/out of MtrF in the cellular MtrDEF complex.

A simple explanation of the observed redox potentials, e.g., in terms of solvent accessibility, could not be found. For instance, the crystal structure-based solvent accessibilities as reported by Clarke et al.[9] did not show any correlation with our computed redox potentials. The use of molecular simulation allows us to analyze the redox potentials in terms of contributions of individual residues by calculating the contribution of each residue to the redox potential of each heme (see SI and Table S3). We find that every charged residue in the environment of a cofactor contributes several tenths of volts, with positively charged residues largely canceling the contribution of negatively charged ones. Although this does not enable a simple explanation of the redox potentials, we highlight in the following a few particularly important residues which are depicted in the insets of Figure 2a and indicated in Figure 2b.

We find that the axial histidine ligands of the hemes with the lowest redox potentials, hemes 4 and 9, form a hydrogen bond with the propionate groups (Prp 5 and Prp10) of the neighboring hemes (5 and 10, respectively). The proprionates are already in the proximity of the histidines in the crystal structure (O−N = 3.24 and 4.85 Å, respectively) and form temporary hydrogen bonds during the dynamics. As can be seen from Figure 2b, there are no positively charged residues in the immediate neighborhood of hemes 4 and 9 that would compensate for the presence of the propionates. This gives a rationale for the relatively high free energy of reduced hemes 4 and 9.

Conversely, the low free energy of reduced heme 7 results from a high density of positively charged residues in its vicinity, including arginine 488 and a doubly protonated histidine nearby (labeled Hip451 in Figure 2b). The latter forms a hydrogen bond with a close-by aspartate in the crystal structure and was thus assumed to be protonated. The empirical pK_a estimation tool propKa[23] gives an estimated pK_a = 7.74 for this residue. This would mean that at pH 7 the fraction of singly protonated (neutral) histidine 451 is 0.15. Scaling the free energy contributions of Hip451 to the heme redox potentials accordingly by a factor of 0.85, both the potential of heme 7 and the range of redox potentials would decrease by ∼60 mV. This suggests that partial deprotonation of histidine 451 will reduce the computed redox potentials to a range in better agreement with experiment, as well as alleviate the role of heme 7 as an electron sink.

Heme 2 is surrounded by negative and positive residues alike. Aspartate 228 remains close to one of the axial histidines of heme 2 (O−H ≈ 2.5 Å most of the time). But in contrast to hemes 4 and 9, there are several positively charged residues in the neighborhood of heme 2, two of which are indicated in Figure 2b (lysines 222 and 237). This provides an explanation for the relatively high redox potential of heme 2 despite the presence of an aspartate nearby.

The free energy landscape for electron flow through the bacterial deca-heme cytochrome MtrF has been calculated via thermodynamic integration, revealing a nearly symmetric profile that can be rationalized by the electrostatic effects of neighboring protein residues. We hope that future experiments will be able to verify some of our predictions. In particular, it would be interesting to see if the introduction of positively charged residues close to the low-potential hemes 4 and 9 could increase their redox potential, which, according to our calculations, would lead to a smaller range of observed redox potentials and a reduction of the two highest barriers for ET, possibly accompanied by an increase in the overall rate for

dx.doi.org/10.1021/ja3027696 | J. Am. Chem. Soc. 2012, 134, 9868−9871

electron transport through the protein. The opposite is expected if more negatively charged side chains were introduced. The next objective in terms of computations is the prediction of rates for ET along the heme chains, which will require estimates of reorganization free energies and electronic coupling elements, both presently underway using molecular simulation.

■ ASSOCIATED CONTENT

Supporting Information

Thermodynamic integration and MD simulation protocols; data evaluation; discussion of interactions with substrates; complete refs 1, 5, 9, and 21. This material is available free of charge via the Internet at http://pubs.acs.org.

■ AUTHOR INFORMATION

Corresponding Author

j.blumberger@ucl.ac.uk; kevin.rosso@pnnl.gov

Notes

The authors declare no competing financial interest.

■ ACKNOWLEDGMENTS

M.B. gratefully acknowledges an IMPACT studentship co-sponsored by University College London and Pacific Northwest National Laboratory (PNNL) through the U.S. Department of Energy's Subsurface Biogeochemistry Research Science Focus Area (SBR-SFA) program of the Office of Biological and Environmental Research, the latter of which provided support for K.R. and P.Z. J.B. thanks the Royal Society for a University Research Fellowship. This work was carried out on HECToR (Edinburgh), to which access was granted via the Materials Chemistry Consortium (EPSRC grant EP/F067496), and on Chinook at EMSL, a national scientific user facility sponsored by the Department of Energy's Office of Biological and Environmental Research and located at Pacific Northwest National Laboratory.

■ REFERENCES

(1) Hartshorne, R. S.; et al. *Proc. Natl. Acad. Sci. U.S.A.* **2009**, *106*, 22169.
(2) Straub, K. L.; Benz, M.; Schink, B. *FEMS Microbiol. Ecol.* **2001**, *34*, 181.
(3) Myers, C. R.; Nealson, K. H. *Science* **1988**, *240*, 1319.
(4) El-Naggar, M. Y.; Wanger, G.; Leung, K. M.; Yuzvinsky, T. D.; Southam, G.; Yang, J.; Lau, W. M.; Nealson, K. H.; Gorby, Y. A. *Proc. Natl. Acad. Sci. U.S.A.* **2010**, *107*, 18127.
(5) Gorby, Y. A.; et al. *Proc. Natl. Acad. Sci. U.S.A.* **2006**, *103*, 11358.
(6) Polizzi, N. F.; Skourtis, S. S.; Beratan, D. N. *Faraday Discuss.* **2012**, *155*, 43.
(7) Xiong, Y. J.; Shi, L.; Chen, B. W.; Mayer, M. U.; Lower, B. H.; Londer, Y.; Bose, S.; Hochella, M. F.; Fredrickson, J. K.; Squier, T. C. *J. Am. Chem. Soc.* **2006**, *128*, 13978.
(8) Jensen, H. M.; Albers, A. E.; Malley, K. R.; Londer, Y. Y.; Cohen, B. E.; Helms, B. A.; Weigele, P.; Groves, J. T.; Ajo-Franklin, C. M. *Proc. Natl. Acad. Sci. U.S.A.* **2010**, *107*, 19213.
(9) Clarke, T. A.; et al. *Proc. Natl. Acad. Sci. U.S.A.* **2011**, *108*, 9384.
(10) Mao, J.; Hauser, K.; Gunner, M. R. *Biochemistry* **2003**, *42*, 9829.
(11) Alfonso-Prieto, M.; Oberhofer, H.; Klein, M. L.; Rovira, C.; Blumberger, J. *J. Am. Chem. Soc.* **2011**, *133*, 4285.
(12) Muegge, I.; Qi, P. X.; Wand, A. J.; Chu, Z. T.; Warshel, A. *J. Phys. Chem. B* **1997**, *101*, 825.
(13) Simonson, T. *Proc. Natl. Acad. Sci. U.S.A.* **2002**, *99*, 6544.
(14) Bortolotti, C. A.; Siwko, M. E.; Castellini, E.; Ranieri, A.; Sola, M.; Corni, S. *J. Phys. Chem. Lett.* **2011**, *2*, 1761.
(15) Blumberger, J.; Klein, M. L. *J. Am. Chem. Soc.* **2006**, *128*, 13854.
(16) Blumberger, J. *Phys. Chem. Chem. Phys.* **2008**, *10*, 5651.
(17) Tipmanee, V.; Oberhofer, H.; Park, M.; Kim, K. S.; Blumberger, J. *J. Am. Chem. Soc.* **2010**, *132*, 17032.
(18) Tipmanee, V.; Blumberger, J. *J. Phys. Chem. B* **2012**, *116*, 1876.
(19) Prytkova, T. R.; Kurnikov, I. V.; Beratan, D. N. *Science* **2007**, *315*, 622.
(20) Skourtis, S.; Balabin, I.; Kawatsu, T.; Beratan, D. *Proc. Natl. Acad. Sci. U.S.A.* **2005**, *102*, 3552.
(21) Case, D. A.; et al. *AMBER 10*; University of California, San Francisco, 2008.
(22) Seidel, R.; Faubel, M.; Winter, B.; Blumberger, J. *J. Am. Chem. Soc.* **2009**, *131*, 16127.
(23) Sondergaard, C. R.; Olsson, M. H. M.; Rostkowski, M.; Jensen, J. H. *J. Chem. Theory Comput.* **2011**, *7*, 2284.